

# Simulation results comparing constant and variable thickness lead plates in the electromagnetic endcap calorimeter

Christine V. Scheel  
*Universidad Autónoma de Madrid, Spain*

## Abstract

The electromagnetic endcap calorimeter is simulated using two alternative designs, one with a constant lead thickness of 1.6 mm, the other with a thickness varying linearly with radius from 1.1 to 2.6 mm. Simulation results of the energy resolution and linearity for the two designs are presented and compared. Both designs produce similar results, with an intrinsic energy resolution of  $\sim 8\%/\sqrt{E} \pm 0.2\%$  and linearity to within 0.5%.

## 1 Introduction

The liquid argon accordion design for the electromagnetic (EM) endcap calorimeter (often called the “Spanish fan”) consists of pleated lead plates extending radially around the beam axis, interleaved with kapton anode layers. An outer “wheel” covers  $1.4 < |\eta| < 2.4$ , the inner  $2.4 < |\eta| < 3.2$ . Details and drawings can be found in ref. [1, 2, 3].

The signal  $S$  from such a calorimeter is a function of several factors:

$$S \propto f_{\text{samp}} \frac{v_d}{g}, \quad (1)$$

where  $f_{\text{samp}}$  is the sampling fraction of the calorimeter,  $v_d$  is the drift velocity of electrons in liquid argon, and  $g$  is the argon gap width. Since  $v_d$  is a function of the electric field  $E$  across the gap, varying as  $E^{0.3}$ , and  $E$  is a function of the high voltage  $U$  and the gap size, with  $E = U/g$ , eq. 1 can be rewritten in terms of design parameters:

$$S \propto \frac{f_{\text{samp}}}{g^{1.3}} U^{0.3}. \quad (2)$$

To avoid additional fluctuations due to non-uniformity, the calorimeter signal should not depend on the impact point of the particle, and so the above expression should be constant over all positions.

The original design for the EM endcap required that the lead plates increase in thickness with increasing radius (and increasing gap size), in order to keep the sampling fraction constant [2]. The value of  $U$  would then be adjusted

to compensate for the increasing gap size with radius. To compensate for a doubling of the signal over the rapidity range of the outer wheel, the high voltage must decrease by  $1/6$ . A prototype was built according to this design and demonstrated, consistent with simulation results, that the design worked as expected [4]. The biggest problem with this design is that the range of HV values required would not be technically practical. Lowering the ADC gain at low rapidity would also be necessary in that case.

The alternative design calls for lead plates with a uniform thickness, allowing a varying  $f_{\text{samp}}$  which is partially compensated by  $g$ , so that the signal in the outer wheel changes by only 25% with  $\eta$ . A variation of  $U$  by a factor of 2.5 can then be introduced to make the signal uniform. The design and some simulation results are found in [3]. The main advantages to this design is the a smaller range in HV needed along the  $\eta$  direction. In fact, since the change in signal is quite small, perhaps a constant high voltage can be used and the non-uniformity corrected in the reconstruction software. It may also be easier to produce high quality lead plates with a constant thickness, depending on the method of smoothing the surface of a plate.<sup>1</sup> The biggest disadvantage is that the total thickness of the calorimeter would be  $25X_0$  or less at low rapidity ( $\eta < 1.7$ ), allowing some shower leakage. However, a large amount of dead material in front in ATLAS in this area will make up for this, and will anyway deteriorate the energy resolution. In all other aspects, the design is similar or the same to the original design.

Many aspects of the two designs options were considered, including cost, mechanical feasibility, and performance in order to choose the final design. Without the time and money to make a second prototype, the last criterion was considered based on simulation results with some well-tested programs. Ref. [2] and [3] give some results based on analytic calculation and on Monte Carlo simulations of electrons of 100 GeV, but without a determination of the energy resolution as a function of energy which would give accurate measurements of the sampling and constant terms. The purpose of the following study was in particular to see how the constant term of the energy resolution compares, using the same simulation programs. The linearity of the signal with energy was also checked. A description of this study and the results are given in the next section (sect. 2). At the end in sect. 3, conclusions are drawn from the study.

## 2 Studies with DICE95 program

### 2.1 Geometry description in DICE95

This study uses GEANT in the DICE95 [5] framework for the simulation of both versions of the entire EM endcap. All the materials and shapes are described, as in ref. [2, 3]. However, the electric field over the liquid argon gap, and hence the charge transport and collection, is not included. Instead, the signal is taken

---

<sup>1</sup>If the plates are machined to obtain a very smooth surface (with an RMS spread of 10  $\mu\text{m}$ , for example), the same effort (and cost) is required for both design options. “Rolling” the plates smooth is only feasible with plates of constant thickness.

to be

$$S = \frac{E_{\text{LAR}}}{g^{1.3}}, \quad (3)$$

where  $E_{\text{LAR}}$  is the energy deposit in the active material which is proportional to  $f_{\text{samp}}$ .<sup>2</sup> There is no simulation of the changing HV ( $U$  in eq. 2) with respect to rapidity, so the signal varies with position in  $\eta$ . The signals in all cells are summed up: there is no calibration nor clustering of cells. No electronic noise or pile-up noise is simulated, so there should be no  $E^{-1}$  noise term in the energy resolution.

## 2.2 Generated particles

Electrons of 10, 50, 100, and 200 GeV were generated at several rapidities: 1.6, 2.0, and 2.2 in the outer wheel and 2.8 in the inner wheel. The particles were generated over a range of 1.5 cells in the azimuthal ( $\phi$ ) direction, where each cell is composed of 3 absorber+gap layers.

## 2.3 Results

Some corrections were made to the signal before determining the energy resolution. There was a small amount of leakage in the back of the calorimeter (typically 0.5% at 10 GeV). It can be corrected for by taking the energy deposit in all materials of the calorimeter and comparing it with the generated energy of the incident particle. Without this correction, the energy resolution is the same within the statistical uncertainty, except at  $\eta = 1.6$  for the constant thickness plates where the calorimeter depth is too short to contain the full shower (as discussed in sect. 1).

A large contribution to the constant term of the energy resolution is the signal modulation with  $\phi$ , resulting from the local differences in the amount of absorber traversed by the shower particles. The parameters which describe the absorber shape and positioning were optimized in order to minimize this non-uniformity in the region  $1.6 < |\eta| < 3.0$  [3]. In order to correct for this periodic effect, a fit was made to the 100 GeV or 200 GeV signal for each rapidity signal as a function of the generated  $\phi$  value, as shown in fig. 1. The function fitted is

$$S = p_1 \left\{ 1 + p_2 \cos(2\pi\phi) + p_3 \exp \left[ -\frac{1}{2} \left( \frac{\phi - 0.5}{p_4} \right)^2 \right] \right\}, \quad (4)$$

where  $p_1$  to  $p_4$  are the fitted parameters [3]. The result of this fit was then used to smooth out the  $\phi$  modulation, as shown in the example in fig. 2. The same correction parameters were used for all energies at a given rapidity, but at low energies high sampling fluctuations dominate and the variation with  $\phi$  is not so apparent. Note that these corrections were made using the generated  $\phi$  position, not the reconstructed one.

With these corrections applied, the signal distribution was fit to a Gaussian shape over the region  $\pm 4\sigma_{\text{RMS}}$  around the mean (which usually encompassed all

---

<sup>2</sup>The charge collection has now been put into the routine and will be checked, but previous studies have indicated that the results should be very similar.

events) to get the mean energy, the resolution, and their corresponding errors (fig. 2). The energy resolution as a function of energy, as seen in fig. 3 and 4, was then fit according to

$$\frac{\sigma_S}{S} = \frac{a}{\sqrt{E}} \oplus b, \quad (5)$$

where  $E$  is the generated energy in GeV. Results are shown for  $a$  and  $b$  using the two geometry designs as a function of  $\eta$  in fig. 5, and listed in table 1.

$\eta$	variable		constant	
	a [%]	b [%]	a [%]	b [%]
1.6	$7.99 \pm 0.48$	$0.48 \pm 0.07$	$7.20 \pm 0.24$	$0.24 \pm 0.79$
2.0	$8.19 \pm 0.25$	$0.18 \pm 0.13$	$8.17 \pm 0.29$	$0.19 \pm 0.14$
2.2	$8.23 \pm 0.38$	$0.19 \pm 0.15$	$8.15 \pm 0.30$	$0.15 \pm 0.17$
2.8	$6.74 \pm 0.36$	$0.20 \pm 0.13$	$7.90 \pm 0.23$	$0.00 \pm 0.15$

Table 1: *The energy resolution with variable thickness lead plates and with constant thickness plates. Corrections for leakage and  $\phi$  modulation have been applied.*

The results for the two geometry options are similar. The sampling term is around  $7 - 8\%/\sqrt{E}$ , below the target value of  $10\%/\sqrt{E}$  [1]. However, when all the realistic parameters, such as clustering and dead material, are included, this term will increase. Only in the inner wheel is there a significant difference, with the constant thickness design having a larger sampling term. This term is still consistent with the values in the outer wheel. The constant term remains at roughly 0.2% throughout the  $\eta$  range for both designs. This residual term is due to the changing signal (in the radial direction) over the depth of the shower which develops in the  $\eta$  direction. At  $\eta = 1.6$ , however, the constant term is twice as large with the variable thickness. In general, the energy resolution for the calorimeter with constant thickness lead plates is either better or the same as with variable thickness plates in the outer wheel.

Also shown on fig. 5 (the circles) is the resolution without the  $\phi$  correction. The signal modulation with  $\phi$  contributes only to the constant term, as expected for such a non-uniformity in position, and the value of this term depends strongly on the rapidity. The correction makes this term practically constant with  $\eta$ , providing a more uniform energy resolution at high energy.

In fig. 6 and 7, the ratio of the signal to energy, normalized to the 100 GeV point, shows that the calorimeter response is almost completely linear with energy. The endcap with constant thickness absorber plates has a slightly more linear response, but, with either design, the signal does not change more than 0.5%. Similar results were found with the prototype in the test beam [4].

### 3 Discussion and conclusions

This study determines the ideal performance of the EM endcap calorimeter. To get an accurate determination of the energy resolution that can be expected under realistic conditions, it is necessary to include other factors that will degrade the resolution, but which are mostly independent of whether the absorber plates vary or stay constant in the radial thickness. In reality, the energy deposit will only be taken from a small cluster of cells, introducing extra sampling fluctuations. The  $\phi$  correction will not be as accurate when the reconstructed position is used instead of the position of the generated particle, which is only known in simulations. The varying high voltage with  $\eta$  may also degrade the resolution and linearity. A term proportional to  $E^{-1}$  in the energy resolution will result from the electronic noise and pile-up events. Extra material in front of the calorimeter will cause some degradation as well. Finally, the calorimeter will never be built perfectly, so remaining imperfections and uncertainties in the construction will affect the constant term.

Great care was taken in the choice of design parameters to optimize the performance of the EM endcap accordion calorimeter [2, 3]. This is confirmed by the good energy resolution of approximately  $8\%/\sqrt{E} \pm 0.2\%$  determined by this simulation, either using lead plates of a constant thickness or ones that vary in thickness. Both design options give signals linear within 0.5% with incident energy. Considering only these results, the constant thickness option is perhaps the better choice. The constant term is better at low rapidity, and the signal is slightly more linear with energy. Considering also the technical advantages of having constant thickness plates, this design was chosen. These advantages include a smaller signal variation with  $\eta$  and so requiring less or no HV variation, and perhaps an easier lead plate production with the required tolerance. Both of these could lead to a smaller cost as well.

## References

- [1] ATLAS Collaboration, “ATLAS Technical Proposal,” CERN/LHCC/94-43 (1994).
- [2] A. Chekhtman *et al.*, “The Accordion in the end-cap: geometry and characteristics,” ATLAS Internal Note LARG-NO-4 (1994).
- [3] S. Klimenko *et al.*, “The design of the endcap EM calorimeter with constant thickness of the absorber plates,” ATLAS Internal Note LARG-NO-25 (1995).
- [4] A. Chekhtman *et al.*, “Performance of a liquid argon electromagnetic end-cap calorimeter using an accordion geometry,” ATLAS Internal Note CAL-NO-067 (1995).
- [5] A. Artomonov *et al.*, “DICE-95,” ATLAS Internal Note SOFT/95-14 (1995).

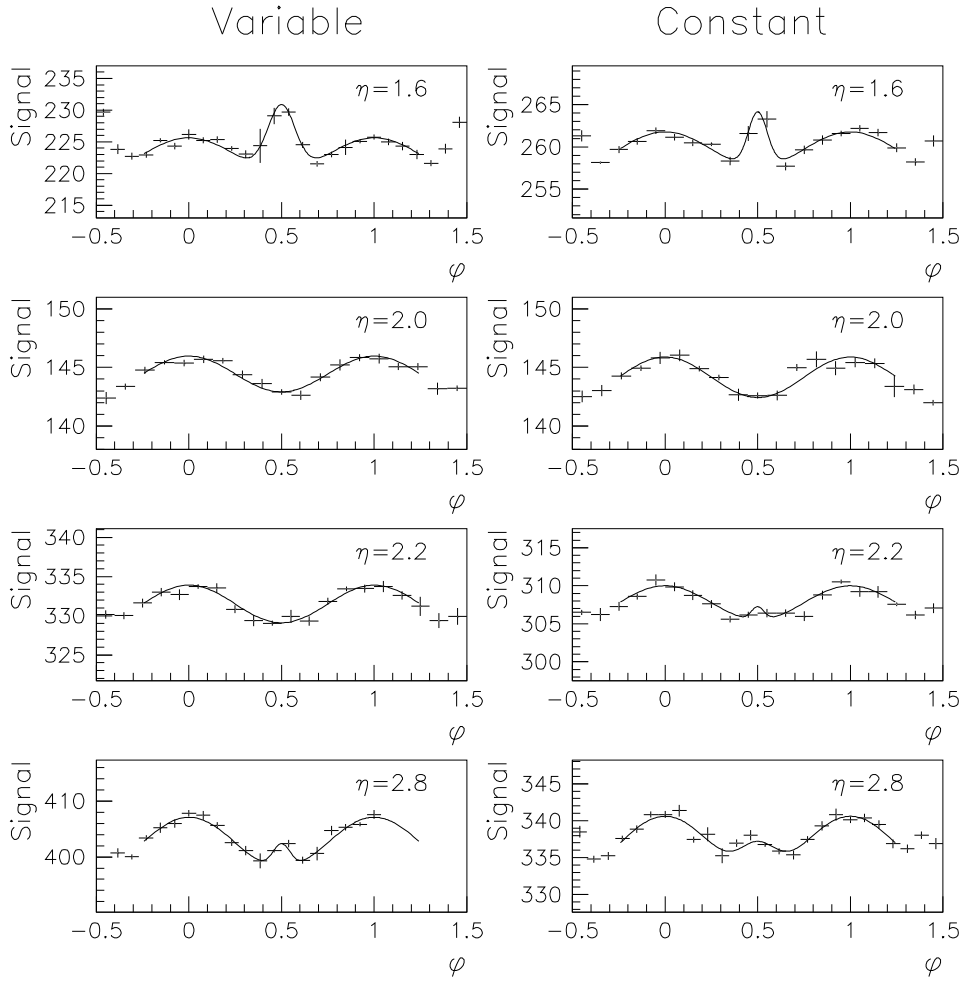


Figure 1: *The signal (in arbitrary units) as a function of the generated azimuthal position (in units of single layers of absorber+kapton) for lead of variable thickness in the left-hand column and of constant thickness in the right-hand column, for several  $\eta$  values. Generated electrons of 200 GeV were used, except at  $\eta = 2.0$ , with 100 GeV electrons. Curves are fits of the form given in eq. 4. Note that the vertical scales is different for each plot.*

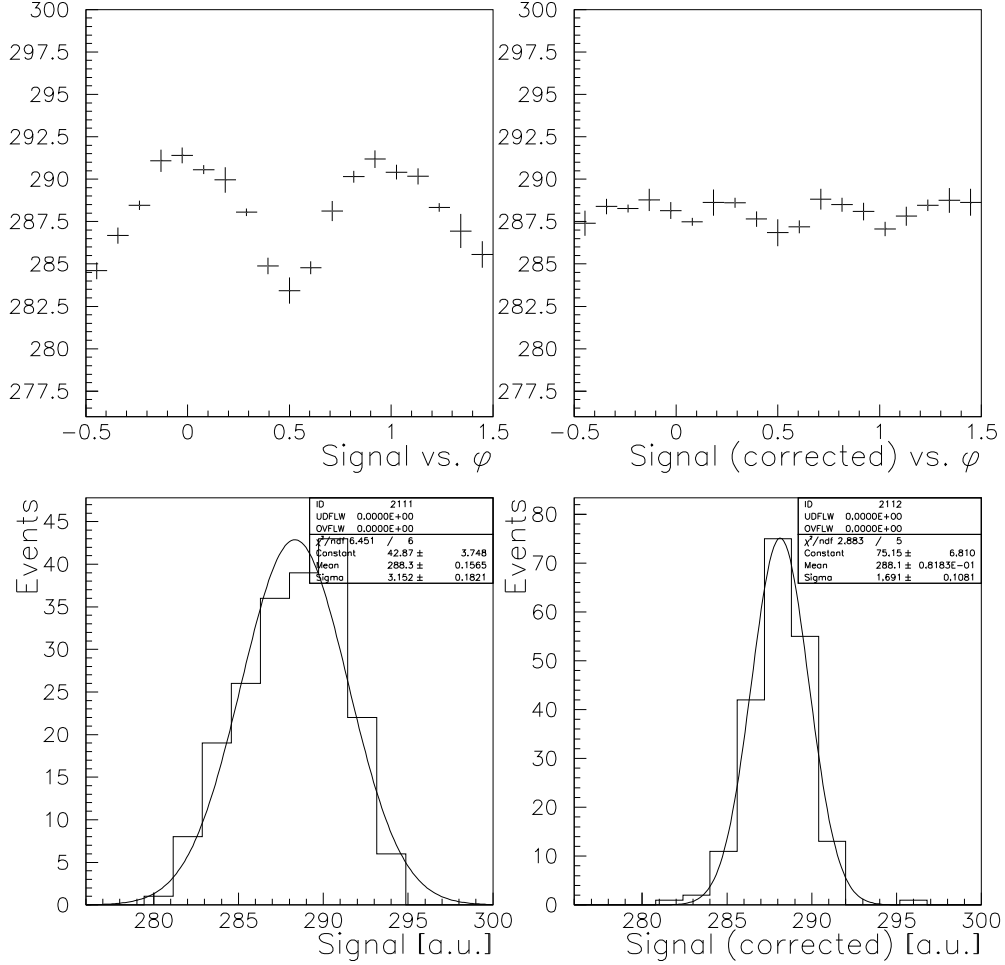


Figure 2: *On the top, the signal (in arbitrary units) as a function of the generated position in  $\phi$  (in units of single layers of absorber+kapton) for lead of constant thickness for  $\eta = 2.0$ , before (left) and after (right) the  $\phi$  correction. Generated electrons of 200 GeV were used. The corresponding signal distributions are shown on the bottom. The curves are Gaussian fits.*



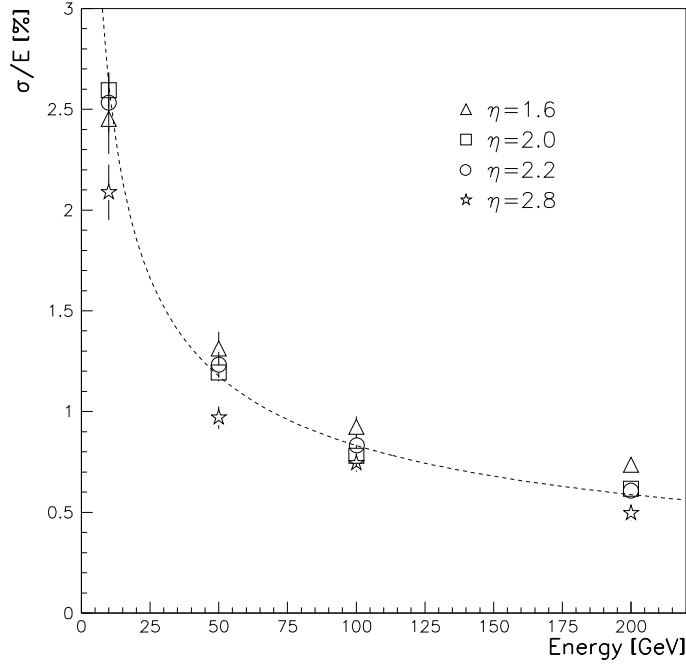


Figure 3: The energy resolution for simulated electrons in the EM endcap with lead plates of variable thickness as a function of the generated energy, at four positions in rapidity. The curve is the best fit to eq. 5 for  $\eta = 2.0$ .

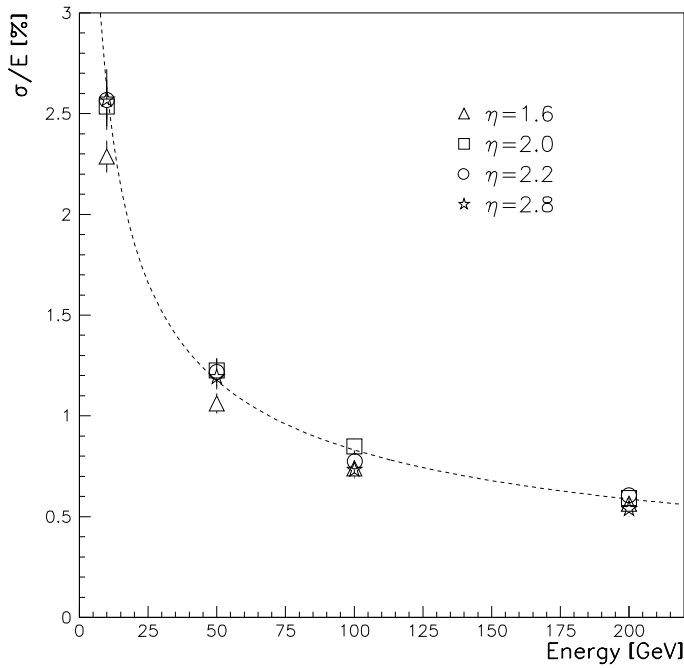


Figure 4: The energy resolution for simulated electrons in the EM endcap with lead plates of constant thickness as a function of the generated energy, at four positions in rapidity. The curve is the best fit to eq. 5 for  $\eta = 2.0$ .

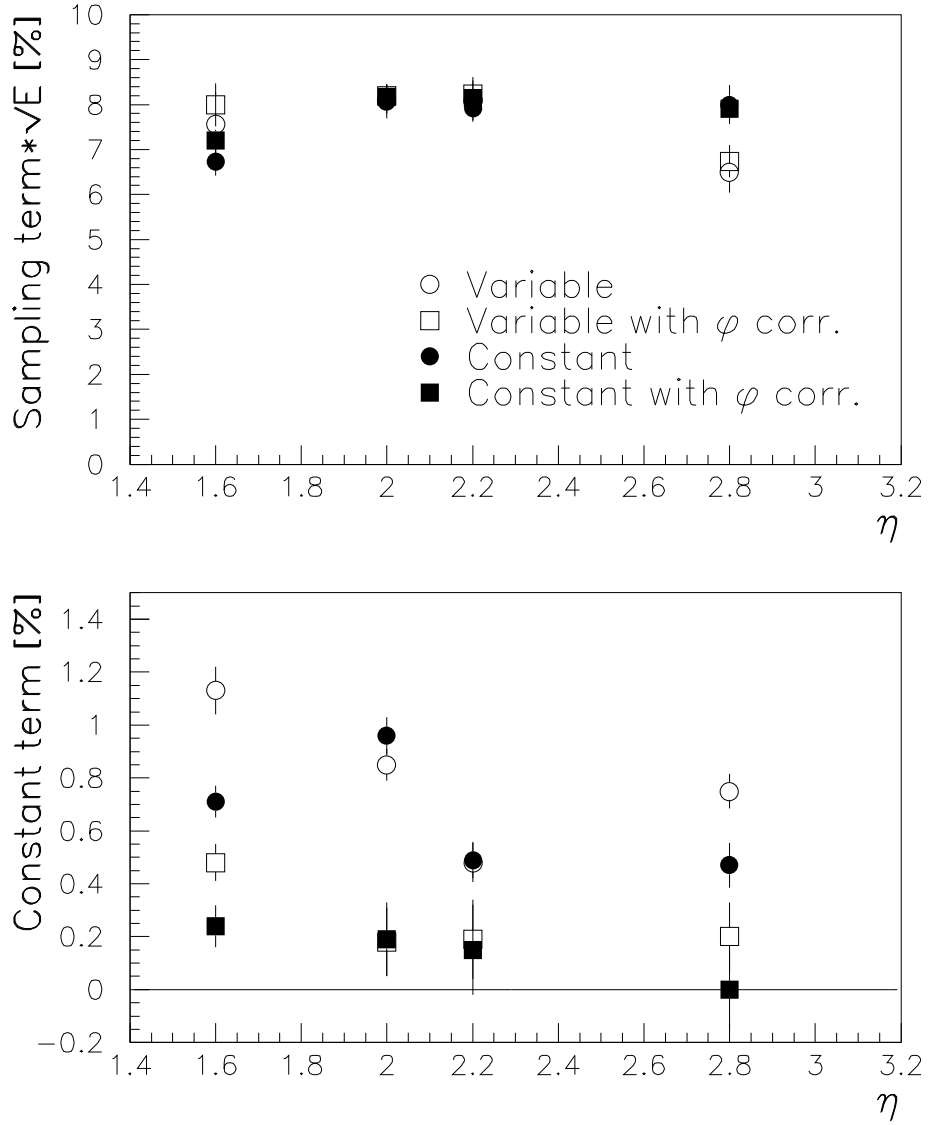


Figure 5: *The coefficient of the sampling term (top) and the constant term (bottom) of the energy resolution as a function of rapidity, for the EM endcap with variable thickness lead plates (open squares) and with constant lead thickness (closed squares). Also shown are the values without the correction for  $\phi$  modulation (open circles and closed circles, respectively).*

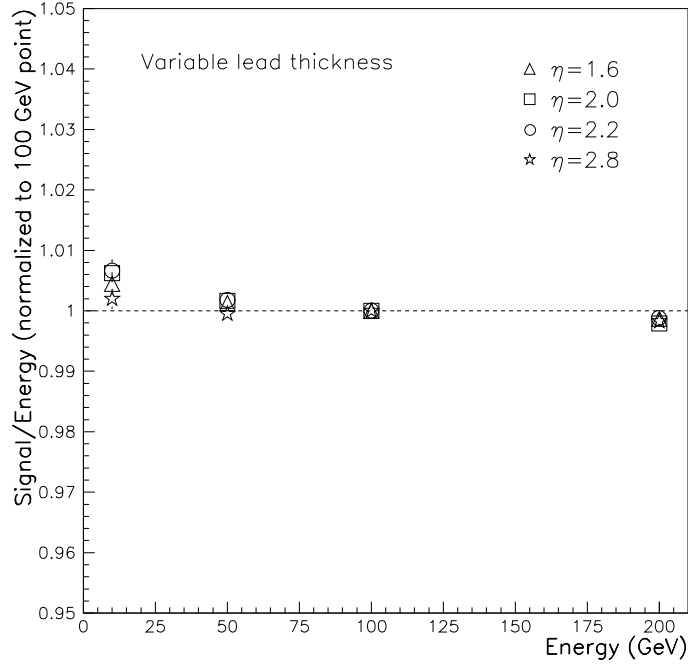


Figure 6: *The signal/energy, normalized to the 100 GeV point at each rapidity, as a function of the generated energy, for simulated electrons in the EM endcap with lead plates of variable thickness at four positions in rapidity.*

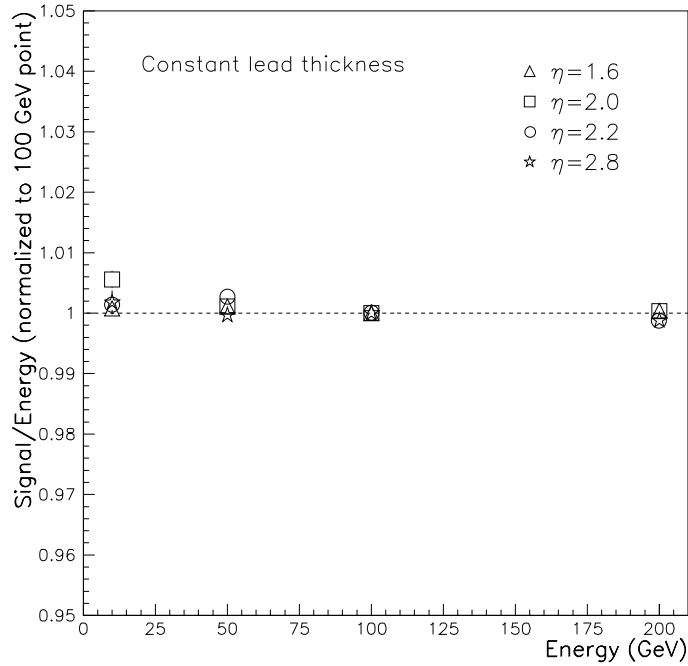


Figure 7: *The signal/energy, normalized to the 100 GeV point at each rapidity, as a function of the generated energy, for simulated electrons in the EM endcap with lead plates of constant thickness at four positions in rapidity.*